Check for updates

Bioelectromagnetics

WILEY

BioEM

Research Article

Radiofrequency Induced Time-Dependent Alterations in Gene Expression and Apoptosis in Glioblastoma Cell Line

Mehmet Zahid Tuysuz[1] | Handan Kayhan[2] | Atiye Seda Yar Saglam[3] | Fatih Senturk[4] | Emin Umit Bagriacik[5] | Munci Yagci[2] | Ayse Gulnihal Canseven[6]

[1]Department of Biophysics, Faculty of Medicine, Harran University, Sanliurfa, Turkey | [2]Department of Adult Hematology, Faculty of Medicine, Gazi University, Ankara, Turkey | [3]Department of Medical Biology and Genetics, Faculty of Medicine, Gazi University, Ankara, Turkey | [4]Department of Biophysics, Faculty of Medicine, Duzce University, Duzce, Turkey | [5]Department of Immunology, Faculty of Medicine, Gazi University, Ankara, Turkey | [6]Department of Biophysics, Faculty of Medicine, Gazi University, Ankara, Turkey

Correspondence: Mehmet Zahid Tuysuz (mz.tuysuz@harran.edu.tr)

Received: 7 May 2024 | **Revised:** 26 November 2024 | **Accepted:** 2 January 2025

Funding: The authors received no specific funding for this work.

Keywords: apoptosis | glioblastoma | nonionizing radiation | radiofrequency electromagnetic fields | RF-EMF

ABSTRACT

The widespread use of wireless communication technologies has increased human exposure to radiofrequency electromagnetic fields (RF-EMFs). Considering the brain's close proximity to mobile phones and its entirely electrical transmission network, it emerges as the organ most profoundly impacted by the RF field. This study aims to investigate the potential effects of RF radiation on cell viability, apoptosis, and gene expressions in glioblastoma cells (U118-MG) at different exposure times (1, 24, and 48 h). To achieve this, we designed and implemented an in vitro RF exposure system operating at a frequency of 2.1 GHz, specifically for cell culture studies, with an average specific absorption rate (SAR) of 1.12 ± 0.18 W/kg determined through numerical dosimetry calculations. Results reveal a significant influence of a 48 h exposure to a 2.1 GHz RF field on U118-MG cell viability, gene expression, and the induction of caspase (*CASP*) dependent apoptosis. Notably, increased *CASP3*, *CASP8*, and *CASP9* mRNA levels were observed after 24 and 48 h of RF treatment. However, only the 48 h RF exposure resulted in apoptotic cell death and a significant elevation in the *BAX/BCL-2* ratio. This observed effect may be influenced by extended exposure durations surpassing the cell's doubling time. The increased *BAX/BCL-2* ratio, which acts as a key switch for apoptosis, and the heterogeneous morphology of the astrocyte-derived U118-MG cell line may also play a role in this effect.

1 | Introduction

The biological effects of radiofrequency electromagnetic fields (RF-EMFs) can be assessed from two distinctive viewpoints based on the areas of study and research objectives. The first perspective is associated with therapeutic applications, which involve short and controlled usage of RF-EMF exposure, including magnetic nano hyperthermia (Senturk 2023; Senturk et al. 2021), tumor treating fields (Stupp et al. 2017), and pulsed electromagnetic field applications (Overholt et al. 2019). The second perspective addresses public health considerations, which pertain to the long-term effects of uncontrolled RF-EMF exposure in real-life environments (Shih et al. 2021). To clarify, when examining the biological effects of frequencies associated with newer technologies like WiFi, LTE, 5G, and WiMAX emitted by mobile phones and widely used wireless communication systems (Tuysuz 2014), the attention shifts toward the domain of public health (Bhatt et al. 2016).

The widespread adoption of wireless and cellular communication technologies, mobile phones, and base stations has resulted in a substantial increase in RF-EMF exposure among the

© 2025 *Bioelectromagnetics* Society.

Summary

- mRNA levels of CASP3, CASP8, and CASP9 increased after 24 and 48 h of RF exposure.
- A statistically significant increase in the BAX/BCL-2 ratio, acting like a switch that allows apoptosis, was only observed after 48 h of RF exposure.
- The apoptotic effects of RF may be influenced by RF exposure times exceeding the cell's doubling time and the heterogeneous morphology of the astrocyte-derived U118-MG cell line.

human population. Numerous studies have explored the potential effects of RF exposure on human health, particularly emphasizing its impact on the brain. These investigations have examined various topics, including the potential thermal consequences resulting from RF energy absorption and the non-thermal effects that may emerge from prolonged RF radiation exposure (Hao et al. 2022). Notably, the proximity of mobile phones to the head exposes the human brain to higher specific absorption rate (SAR) values than other organs in the body, thereby raising concerns about the potential health risks associated with RF exposure.

Numerous experimental studies have demonstrated that RF field exposure can trigger diverse biological responses, including apoptosis (Liu et al. 2012), autophagy (Zielinski et al. 2020), DNA damage (Xu et al. 2013), proinflammatory reactions (Lu et al. 2014), oxidative stress (Georgiou and Margaritis 2021; Schuermann and Mevissen 2021), and alterations in gene expression (Zhao, Zou, and Knapp 2007). Specifically, RF exposure has been demonstrated to affect apoptosis-related markers, including proapoptotic proteins like BAX and CASP, alongside antiapoptotic markers such as BCL-2. For instance, a significant increase in BAX expression, coupled with a decrease in BCL-2 levels, was observed following 1950 MHz RF exposure (Liu et al. 2012). This proapoptotic shift was further supported by the upregulation of CASP2 and CASP6 under similar conditions (Zhao, Zou, and Knapp 2007).

In contrast, several studies have reported no discernible biological effects following RF field exposure (Chauhan et al. 2007; Joushomme et al. 2022; Kayhan et al. 2016; Liu et al. 2015; de Gannes et al. 2011; Sekijima et al. 2010). For instance, no significant changes in apoptosis markers were found in glioblastoma and glial cells exposed to 1.9 and 2.45 GHz RF fields, respectively (Qutob et al. 2006; Sakurai et al. 2011). Further studies on glioblastoma (Hirose et al. 2006) and neuroglioma (Sekijima et al. 2010) cells also reported no significant alterations in apoptotic mRNA levels under 2.1 GHz RF exposure. However, while experimental studies show controversial results on the biological effects of RF field exposure, epidemiological studies have pointed to an elevated risk of gliomas (Boyle and Levin 2008; Hardell, Carlberg, and Hansson Mild 2013; Lahkola et al. 2007). The International Agency for Research on Cancer (IARC) has classed radiofrequency (RF) fields as possibly carcinogenic (Group 2B) for humans based on findings from epidemiological research (Baan et al. 2011). Despite the heightened cancer risk underscored by epidemiological findings, the experimental research on the effects and mechanisms of RF radiation remains characterized by inconsistencies and limited insights. This underscores the urgent need for novel experiments designed to elucidate how various cell types respond to RF exposure and to evaluate their sensitivities comprehensively.

This study aims to investigate the impact of RF field exposure on cell viability, apoptosis, and gene expression in the U118-MG human glioblastoma cell line. In this regard, glioblastoma cell lines were exposed to an RF field with a frequency of 2.1 GHz over intervals of 1, 24, and 48 h. To achieve this, we employed numerical calculations to design the RF exposure system and evaluate the specific absorption rate (SAR) distribution within the cell culture samples. To our knowledge, the U118-MG cell line, a type of glial cell cancer associated with an increased risk according to epidemiological studies, was investigated for the first time for mobile phone-specific RF field exposure experiments.

2 | Materials and Methods

2.1 | RF Exposure System

The in vitro RF exposure system was designed and manufactured to expose cell cultures simultaneously to a 2.1 GHz RF electromagnetic field within controlled environmental and electromagnetic conditions (Figure 1). The system was designed to achieve homogeneity among the samples, eliminate hot spots, and ensure optimal ventilation for high-quality experiments.

The in vitro RF field exposure system was constructed using aluminum material. It was chosen for its RF shielding properties and ability to absorb and dissipate heat generated within the exposure system efficiently (Figure 1a). Furthermore, air holes were strategically placed on both the top and bottom levels of the RF exposure system to serve three purposes. First, they maintained the required environmental conditions (37°C, 5% CO_2, 95% humidity) for cell viability. Second, they facilitated the effective dissipation of heat during experiments. Third, they minimized the amount of RF leakage within the system and decreased the interference caused by external RF fields. To further enhance the ventilation and heat management of this system, we implemented active cooling (Figure 1b). This involved installing a 20 cm diameter fan positioned at the base of the in vitro RF exposure system.

The RF exposure system comprises a two-layer shelf, with each layer containing four 35 mm Petri dishes, allowing for eight Petri dishes to be simultaneously exposed to the RF field (Supporting Information S1: Figures 1 and 2). The system is designed with three layers progressing from the outermost to the innermost: an exterior layer made of aluminum, an intermediate layer featuring RF absorber material (specifically ETS-Lindgren FL-2250CL from Texas, USA), and an innermost layer constructed from plexiglass (Figure 1c). This innovative system has been officially registered with the Turkish Patent Institute (TPE) under the registration number "TR 2016 12016 B" and can be accessed via the following link: https://portal.turkpatent.gov.tr/anonim/arastirma/patent/sonuc/dosya?patentAppNo=2016/12016&documentsTpye=all.

1521186x, 2025, 1, Downloaded from https://onlinelibrary.wiley.com/doi/10.1002/bem.22543 by University Of British Columbia, Wiley Online Library on [10/10/2026]. See the Terms and Conditions (https://onlinelibrary.wiley.com/terms-and-conditions) on Wiley Online Library for rules of use; OA articles are governed by the applicable Creative Commons License

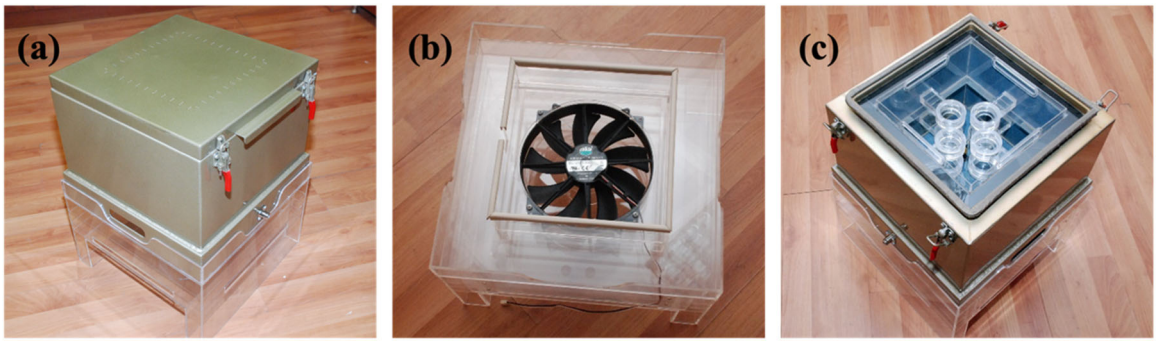


FIGURE 1 | In vitro RF-EMF exposure system, (a) RF exposure system with the ventilation unit (the lid is closed), (b) the top view of the stand-alone ventilation unit, (c) the interior of the RF exposure system with the top and bottom petri dish holders visible when the lid is open.

Our experimental setup comprises an in vitro RF exposure system equipped with a vertical half-wave dipole antenna centrally positioned and connected to a vector signal generator (SMBV100A, Rohde & Schwarz, Munich, Germany), which supplies the 2100 MHz UMTS (3GPP FDD) signal. The dipole antenna, specifically designed for the 2100 MHz RF frequency, has a half-wavelength of 68 mm and is constructed using low-loss Amphenol LMR-240 RF cable, terminated with upTech SMA connectors. The antenna was tested through standing wave ratio (SWR) measurements, yielding a value of 2.0, ensuring minimal signal reflection and optimal power delivery to the system. To maintain optimal cell culture conditions (37°C, 5% CO_2, and 95% humidity), the RF exposure system was placed inside a CO_2 incubator (Nuve EC 160, Ankara, Turkey). The output power from the vector signal generator was set to 23 dBm, generating an electric field intensity of 60 V/m, measured using the Narda EMR-300 device. This configuration ensures consistent and controlled RF exposure conditions, providing a stable and reproducible environment for cellular studies and allowing for precise investigation of RF-induced biological effects.

2.2 | RF Dosimetry

In our study, we employed numerical calculations to design the RF exposure system and assess the SAR distribution within the cell culture samples (Petri dishes). This involved using SEMCAD X software developed by SPEAG in Switzerland, leveraging the finite difference time domain (FDTD) method. To optimize computational efficiency, conformal FDTD and a grading mesh algorithm were applied, leading to reduced voxel count and computation time. The simulation sizes varied, ranging from 40 to 125 million voxels, depending on the specific simulation conditions. The simulation process includes specific components such as aluminum, RF absorbers, and plexiglass materials (Figure 2a). The materials used in the simulation, their geometries, and dielectric properties are modeled in accordance with real conditions. In addition, a mathematical model with a value of 2 mm is used to represent the height of the medium in a 35 mm petri dish. The dielectric properties of the materials used in the simulation were obtained from the literature, with values reported for DMEM and plexiglass (Schuderer et al. 2004) and for the RF absorber (Wang et al. 2008). Metallic components were modeled as perfect electric conductors (PEC). The dielectric characteristics, including permittivity, conductivity, and density, are summarized in Table 1.

In our study, we have provided SAR distribution patterns calculated based on the electric field using the following formula:

$$\mathrm{SAR} = \sigma \frac{E^2}{\rho} (1)$$

In the formula, σ represents the electrical conductivity of the tissue (S/m), E is the root-mean-square electric field (V/m) induced in the tissue, and ρ is the tissue density (kg/m^3). Since SAR (W/kg) is directly related to E^2, the SAR distribution accurately reflects the electric field distribution in the tissue, ensuring a precise understanding of RF energy absorption patterns. Due to the limited liquid volume in the 35 mm Petri dish, which is less than 10 g, the SAR values were calculated based on a mass of 1 g. The 1 g spatial peak SAR represents the maximum rate at which RF energy is absorbed by 1 g of biological tissue, expressed in watts per kilogram (W/kg). This is determined by averaging the spatial peak SAR across any 1 g cube of tissue in the region with the highest RF exposure, providing a crucial measure of localized energy absorption. The 1 g SAR is determined according to the IEC/IEEE 62209-1528:2020 standard, ensuring compliance with international safety and exposure guidelines (IEC/IEEE International Standard).

Figure 2b,c presents the dosimetry results for the 2100 MHz RF-EMF, demonstrating an average SAR value of 1.12 ± 0.18 W/kg for a mass of 1 g. This SAR value corresponds to an incident power of 23 dBm (200 mW) applied during the exposure experiments. Notably, the SAR value of our experimental setup not only matches real-life usage conditions but also complies with established safety guidelines and remains below the recommended values (IEC/IEEE International Standard 2020). This provides strong reassurance about the safety of our experimental setup. Furthermore, temperature variations during RF-EMF exposure were monitored throughout the experiment using an infrared thermal camera (FLIR E6, Sweden), with observations conducted before exposure, after its initiation, and at regular intervals during the exposure period. No discernible temperature increase was observed, confirming the thermal safety of our experimental setup. In the conditions we examined, plexiglass layers acted as a guide for electromagnetic waves and directed them. This was used to increase the RF field homogeneity applied to the samples and eliminate hot spots within the

1521186x, 2025, 1, Downloaded from https://onlinelibrary.wiley.com/doi/10.1002/bem.22543 by University Of British Columbia, Wiley Online Library on [10/10/2026]. See the Terms and Conditions (https://onlinelibrary.wiley.com/terms-and-conditions) on Wiley Online Library for rules of use; OA articles are governed by the applicable Creative Commons License

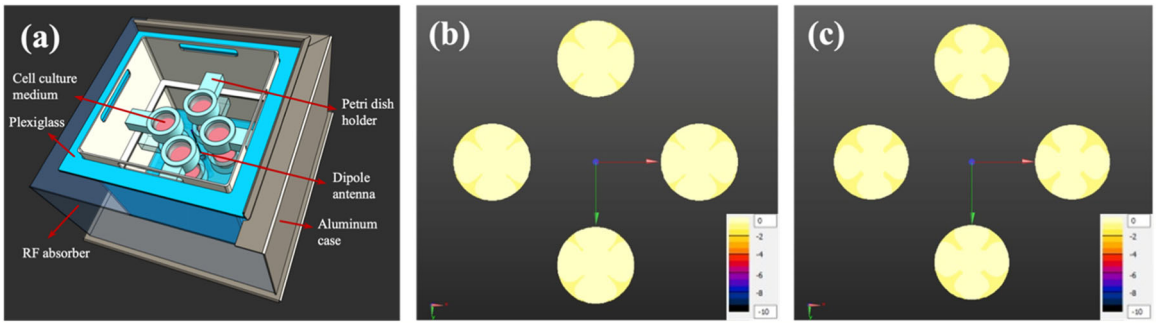


FIGURE 2 | (a) A three-dimensional numerical calculation model of the RF-EMF exposure system, including key components such as the petri dish holders, dipole antenna, aluminum case, RF absorbers, plexiglass, and cell culture medium. (b) Numerical computation of specific absorption rate (SAR) distribution across four Petri dishes in the top layer. (c) Corresponding SAR distribution across four Petri dishes in the bottom layer. The color bar for SAR is reported in a logarithmic scale, considering 1.12 W/kg as the reference value (0 dB = 1.12 W/kg).

TABLE 1 | Dielectric properties of the materials used in the simulation.

Materials	ε_r	σ (S/m)	ρ (kg/m^3)
DMEM	71	2.5	1000
Plexiglass	2.5	0.001	1100
RF absorber	2.3	0,76	70

RF field exposure system. SAR distribution patterns also clearly show this situation for (Figure 2b) the top layer, which includes four Petri dishes, and (Figure 2c) the bottom layer, which also consists of four Petri dishes. We have examined the 2100 MHz SAR distribution data in both the top and bottom Petri dishes. The volume within the ±3 dB range for both the top and bottom layers of the Petri dishes is highly comparable, with the bottom layer accounting for 80.96% and the top layer for 80.52% of the total volume. This ensures homogeneous exposure throughout the setup, supporting the reliability of the SAR distribution across all samples. To further enhance clarity, we have included simulation images normalized to 5, 10, and 20 dB scales in the Supporting Information. These additional visualizations provide a more comprehensive depiction of the field distribution and ensure precision in the analysis (Supporting Information S1: Figure 3).

2.3 | Cell Culture

The human glioblastoma cell line (U118-MG) was obtained from the Department of Immunology at Gazi University Medical Faculty (Ankara, Turkey). This cell line displays a complex morphology, including characteristics of both glioblastoma and astrocytoma cells. The doubling time for U118-MG cells has been determined to be approximately 22 h. U118-MG cells were cultured in Dulbecco's modified Eagle's medium (DMEM) supplemented with 10% (v/v) Fetal Bovine Serum (FBS), 1% (v/v) L-glutamine, and 1% (v/v) penicillin-streptomycin.

2.4 | Cell Exposure Protocol

U118-MG human glioblastoma cells were seeded in 35 mm cell culture dishes (2.5×10^5 cells per dish) and incubated overnight. All incubations were performed at 37°C in a humidified atmosphere, including 5% CO_2. After incubation, the cells were divided into four groups: (i) sham, (ii) 1 h RF exposure, (iii) 24 h RF exposure, and (iv) 48 h RF exposure. The sham group was placed in the exposure system under identical conditions but without the RF field being applied, ensuring control over any external or environmental factors. Also, the necessity of using sham groups in RF field experiments to control for confounding factors and ensure reliable results has been previously emphasized (Cantu et al. 2024). The RF exposure groups were subjected to a 2.1 GHz RF field with a SAR of 1 W/kg for the designated time periods (1, 24, or 48 h). The in vitro RF field exposure system was designed to enable simultaneous RF field exposure of eight 35 mm cell culture dishes in each group (Figure 1a,b). Therefore, eight 35 mm cell culture dishes were placed into the system for each group and exposed to the RF field. The experiments were conducted in a blinded manner, with the RF exposure and subsequent assessments being performed by different individuals to eliminate bias and ensure objective outcome evaluation. After RF exposure periods, cell viability, apoptosis, and related gene expression were determined in U118-MG cells using the methods described in the subsections.

2.4.1 | Cell Viability Assay

Cell viability was determined by the WST-1 cell proliferation reagent (Roche, Basel, Switzerland) according to the manufacturer's instructions. After the RF treatments, the cells were transferred to 96-well plates (1×10^4 cells/well) by trypsinization and incubated overnight at 37°C for attachment. The culture medium was replaced with fresh medium (100 µL) containing 10 µL WST-1 solution in each well, and the cells were incubated for 4 h in a humidified atmosphere (37°C, 5% CO_2). Finally, the absorbance at 450 nm (reference wavelength, 620 nm) was measured by a microplate reader (Tecan-SunRise, Switzerland). Each experiment was performed in triplicate.

2.4.2 | Cell Apoptosis Assay

Cell apoptosis was measured by flow cytometry (FACS, FACSCalibur, BD Biosciences, USA) with a FITC Annexin V Apoptosis Detection Kit I (BD Biosciences, USA) according to the manufacturer's instructions. Briefly, cells were trypsinized and washed twice with ice-cold phosphate-buffered saline (PBS) and then resuspended

1521186x, 2025, 1, Downloaded from https://onlinelibrary.wiley.com/doi/10.1002/bem.22543 by University Of British Columbia, Wiley Online Library on [10/10/2026]. See the Terms and Conditions (https://onlinelibrary.wiley.com/terms-and-conditions) on Wiley Online Library for rules of use; OA articles are governed by the applicable Creative Commons License

at a concentration of 1×10^6 cells/mL in 1X Annexin V Binding Buffer. Then, 100 μL (1×10^5 cells) of the solution was transferred to a 5 mL culture tube, and 5 μL of FITC Annexin V and 5 μL PI were added to the solution. The cells were gently vortexed and incubated for 15 min at room temperature (25°C) in the dark. Then, 400 μL of 1X Annexin V Binding Buffer was added to each tube and analyzed by flow cytometry within 1 h. For FACS analysis, at least 10,000 cells were evaluated in each sample.

2.4.3 | Quantitative Real-Time Polymerase Chain Reaction (qRT-PCR)

The gene expressions of U118-MG human glioblastoma cells were examined by qRT-PCR. Total RNA was extracted from each sample using a High Pure RNA Isolation kit (Roche Diagnostics GmbH) according to the manufacturer's protocol. The total RNA concentration and purity of each sample were quantified using a Nanodrop spectrophotometer (NanoDrop 2000, Thermo Scientific, USA). Subsequently, 1 μg of total RNA was reverse-transcribed into complementary DNA (cDNA) using a Transcriptor First Strand cDNA Synthesis kit (Roche, Mannheim, Germany). The mRNA expression levels of Caspase 3 (*CASP3*), Caspase 8 (*CASP8*), Caspase 9 (*CASP9*), *BCL-2*, *BAX*, CYCLIN D1 (*CYCD1*), *c-MYC*, *c-FOS*, and glyceraldehyde-3-phosphate dehydrogenase (*GAPDH*) were measured by using quantitative real-time PCR with a LightCycler 480 instrument (Roche Diagnostics, Mannheim, Germany). Gene-specific intron spanning primers and probes were designed using the Universal Probe Library (UPL) Assay Design Center (Roche Diagnostics, Mannheim, Germany). The sequences of primers and numbers of UPL probes are shown in Table 2. Thermal cycling conditions consisted of an initial denaturation at 95°C for 10 min, followed by 45 cycles of 10 s at 95°C, 20 s at 60°C, and 30 s at 40°C. To normalize individual gene expression levels, GAPDH was used as an internal control. Each experiment was performed in triplicate.

2.5 | Statistical Analysis

Throughout the paper, the results are expressed as the mean ± SD. To evaluate the statistical significance of cell viability, apoptosis, and gene expression data, non-parametric statistical methods were employed. Pairwise comparisons were conducted using the Mann-Whitney U test, while comparisons across multiple groups were performed using the Kruskal-Wallis test. Fold changes in *CASP3, CASP8, CASP9, BCL-2, BAX, CYCD1, c-MYC*, and *c-FOS* gene expression were calculated using the $2^{-\Delta\Delta Ct}$ method (Livak and Schmittgen 2001 #34), and significant differences in normalized Ct values were identified. The results were considered; ns, $p > 0.05$; $^{*}p < 0.05$, $^{**}p < 0.01$, $^{***}p < 0.001$.

3 | Results

3.1 | Cell Viability

Human glioblastoma cells (U118-MG) were exposed to a 2.1 GHz RF field at a SAR of 1.12 W/kg for varying durations of 1, 24, and 48 h. Following the exposure periods, the viability of glioblastoma cells was determined by colorimetric WST-1 assay. After 1 h and 24 h of RF field exposure, our analysis did not reveal any significant differences in cell viability between the exposed and sham group ($p > 0.05$) (Figure 3a). However, 48 h

TABLE 2 | The primer sequences and probe numbers used for qRT-PCR.

Gene		Primer sequences	UPL Prob Number
GAPDH	Forward	5′- AGCCACATCGCTCAGACAC -3′	60
	Reverse	5′- GCCCAATACGACCAAATCC -3′	
CASP3	Forward	5′- TGGAATTGATGCGTGATGTT -3′	68
	Reverse	5′- TGGCTCAGAAGCACACAAAC -3′	
CASP8	Forward	5′-TCCAAATGCAAACTGGATGA -3′	62
	Reverse	5′- TCCCAGGATGACCCTCTTCT -3′	
CASP9	Forward	5′-CCATATGATCGAGGACATCCA-3′	27
	Reverse	5′-GACTCCCTCGAGTCTCCAGAT-3′	
BCL-2	Forward	5′- AGTACCTGAACCGGCACCT -3′	75
	Reverse	5′- GCCGTACAGTTCCACAAAGG -3′	
BAX	Forward	5′- ATGTTTTCTGACGGCAACTTC -3′	57
	Reverse	5′- ATCAGTTCCGGCACCTTG -3′	
CYCD1	Forward	5′- TGTCCTACTACCGCCTCACA -3′	16
	Reverse	5′- CAGGGCTTCGATCTGCTC -3′	
c-MYC	Forward	5′- GCTGCTTAGACGCTGGATTT -3′	75
	Reverse	5′- CACCGAGTCGTAGTCGAGGT -3′	
c-FOS	Forward	5′- ACTACCACTCACCCGCAGAC -3′	67
	Reverse	5′- CCAGGTCCGTGCAGAAGT -3′	

15231186x, 2025, 1, Downloaded from https://onlinelibrary.wiley.com/doi/10.1002/bem.22543 by University Of British Columbia, Wiley Online Library on [10/10/2026]. See the Terms and Conditions (https://onlinelibrary.wiley.com/terms-and-conditions) on Wiley Online Library for rules of use; OA articles are governed by the applicable Creative Commons License

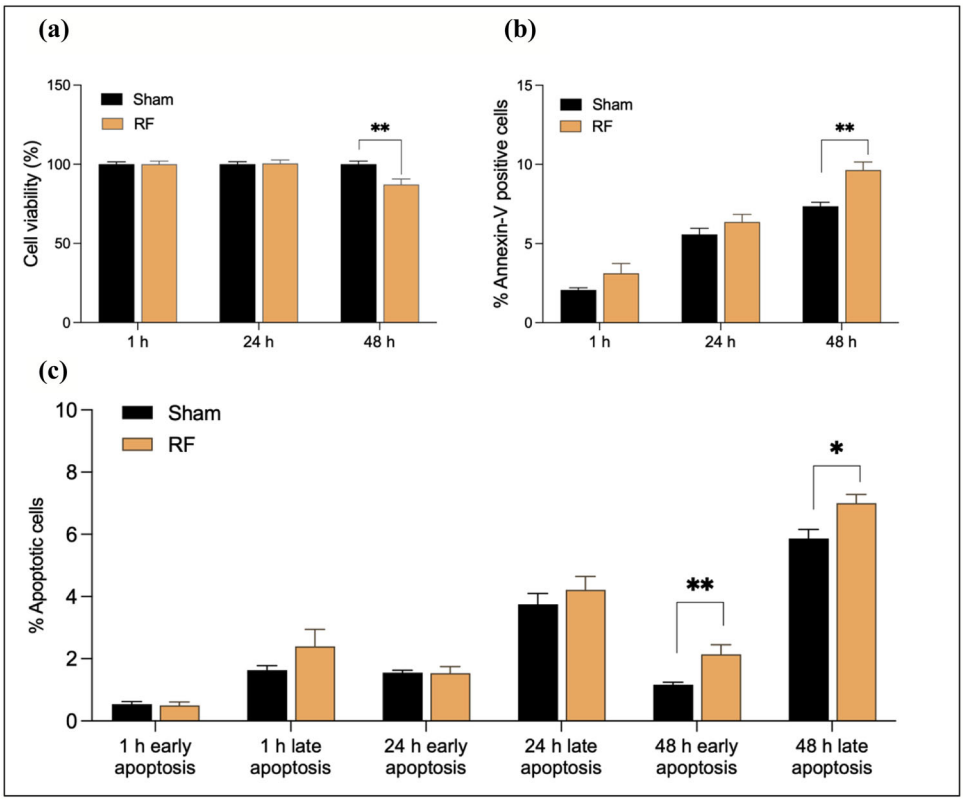


FIGURE 3 | Effects of RF-EMF on (a) cell viability, (b) Annexin-V positive cells, and (c) apoptotic cells (early and late apoptosis) in U118-MG cells. The viability of U118-MG cells was measured using the WST-1 assay. Apoptosis in U118-MG cells was measured by flow cytometry using the Annexin-V-FITC/PI assay. All experiments were carried out with at least three replicates, and the data are represented by the mean ± SD. Non-significant, ns, $p > 0.05$; *$p < 0.05$; **$p < 0.01$; ***$p < 0.001$.

of RF exposure significantly inhibited the viability of U118-MG cells compared to the sham group ($p < 0.01$).

3.2 | Apoptosis (Flow Cytometry)

Apoptosis is related to the loss of membrane asymmetry, leading to the translocation of phosphatidylserine (PS) from the inner to the outer leaflet of the plasma membrane. The use of propidium iodide (PI) and FITC-labeled Annexin V (Annexin V-FITC) is a widely accepted method for assessing apoptosis progression (Wlodkowic et al. 2011). Early apoptotic cells are identified as Annexin V-positive and PI-negative (Annexin V-FITC$^+$/PI$^-$), whereas late apoptotic cells exhibit Annexin V/PI double-positive (Annexin V-FITC$^+$/PI$^+$) staining (Brauchle et al. 2014). To investigate the effect of 2.1 GHz RF field exposure on apoptosis in U118-MG glioblastoma cells, we employed flow cytometry using the Annexin V-FITC/PI assay. Following 1 and 24 h of RF exposure, no statistically significant differences were observed in the number of Annexin V-positive cells compared to the sham-exposed groups (Figure 3b). However, after 48 h of RF exposure, the percentage of Annexin V-positive cells increased significantly to 9.64%, compared to the sham group ($p < 0.01$), indicating an increase in apoptotic activity (Figure 3b). Furthermore, as shown in Figure 3c, after 48 h of RF exposure, the percentage of apoptotic cells was quantified as 2.14% for early apoptosis and 7.00% for late apoptosis. Both early ($p < 0.01$) and late apoptosis ($p < 0.05$) showed statistically significant increases compared to the sham groups. Therefore, our findings demonstrate that prolonged RF exposure (48 h) significantly induces apoptosis in U118-MG cells, both in the early and late stages.

3.3 | Expression of *CASP3, CASP8, CASP9, BAX, BCL-2, CYCD1, c-MYC*, and *c-FOS* mRNA Levels in RF-EMF Exposure to Cells

To evaluate the impact of RF field exposure on proliferative and apoptotic genes within U118-MG cells, we conducted a comprehensive analysis of mRNA levels for *CASP3, CASP8, CASP9, BAX, BCL-2, BAX/BCL-2, CYCD1, c-MYC, and c-FOS* using qRT-PCR (Figure 4). We observed that a 1 h RF field exposure did not produce any significant effect on the expression levels of the *CASP3, CASP8, CASP9*, and *BAX* genes in U118-MG cells compared to the sham groups (Figure 4a–d). However, extending the exposure duration to 24 h resulted in a significant upregulation, with more than a two-fold increase in *CASP3, CASP8, CASP9*, and *BAX* mRNA levels compared to the sham groups. The most notable effects were observed after 48 h of RF exposure in mRNA levels of *CASP3, CASP8, CASP9*, and *BAX* in U118-MG cells, as compared to the sham groups (Figure 4a–d). Specifically, the mRNA level of *CASP8* showed an increase of more than 3.5-fold, while the *CASP3*, *CASP9*, and *BAX* genes demonstrated increases of more than twofold. In addition, *BCL-2* mRNA levels displayed a significant decrease following 48 h of

1521186x, 2025, 1, Downloaded from https://onlinelibrary.wiley.com/doi/10.1002/bem.22543 by University Of British Columbia, Wiley Online Library on [10/10/2026]. See the Terms and Conditions (https://onlinelibrary.wiley.com/terms-and-conditions) on Wiley Online Library for rules of use; OA articles are governed by the applicable Creative Commons License

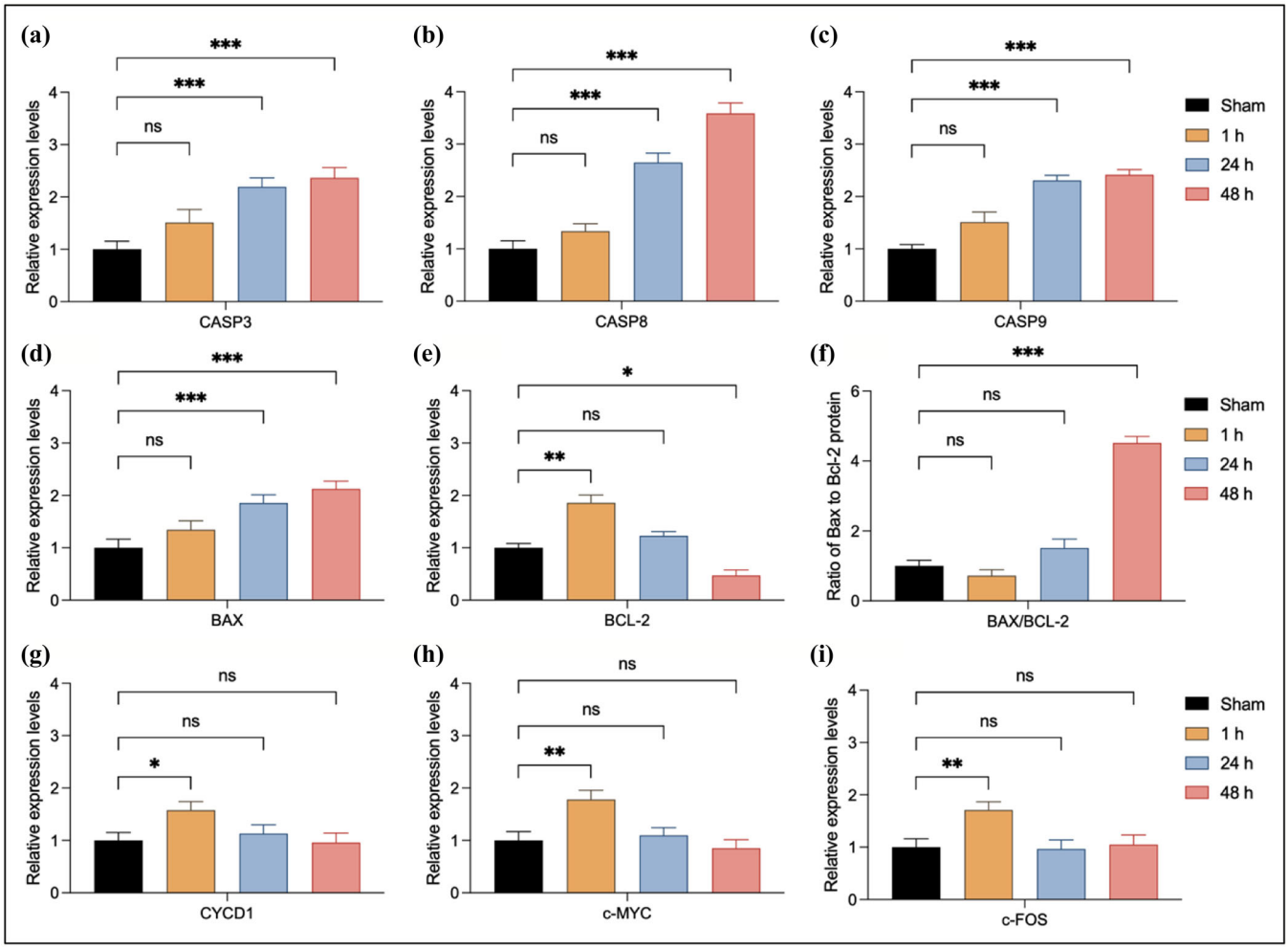


FIGURE 4 | Effects of RF-EMF on mRNA expression levels in U118-MG cells. The expression levels of (a) *CASP3*, (b) *CASP8*, (c) *CASP9*, (d) *BAX*, (e) *BCL-2*, (f) *BAX/BCL-2 ratio*, (g) *CYCD1*, (h) *c-MYC*, and (i) *c-FOS* genes were analyzed following sham and RF-EMF exposure for 1 h, 24 h, and 48 h in U118-MG cells using quantitative real-time PCR (qRT-PCR). Statistical significance was indicated as follows: ns (not significant, $p > 0.05$); *$p < 0.05$; **$p < 0.01$; ***$p < 0.001$.

RF exposure. Furthermore, it is important to note that a statistically significant increase in the *BAX/BCL-2* ratio was only observed after 48 h of exposure ($p < 0.001$) (Figure 4f). On the other hand, *CYCD1* exhibited a statistically significant increase after 1 h of RF application ($p < 0.05$), as depicted in Figure 4g. However, this increase was not observed to be statistically significant following 24 and 48 h of RF application ($p > 0.05$). Similarly, *c-MYC* and *c-FOS* expression levels also displayed significant increases after 1 h of RF application ($p < 0.01$), as shown in Figures 4h,i, respectively. However, no statistically significant changes were evident after 24 and 48 h of continuous RF application for both *c-MYC* and *c-FOS* ($p > 0.05$).

4 | Discussion

The brain stands out as the organ most profoundly affected by the RF field, primarily due to two key factors: its close proximity to mobile phones and its purely electrical transmission network. Considering the brain's regular and extensive interaction with such electronic devices, it seems to exhibit a heightened susceptibility to the possible impacts of RF radiation. The brain is comprised primarily of two types of cells: neurons and glial cells. Some studies have reported that glial cells, particularly astrocytes, possess a higher level of sensitivity to RF fields compared to neurons (Zhao, Zou, and Knapp 2007) and non-astrocytic glioma cells (Liu et al. 2012). Therefore, we used the human glioblastoma cell line U118-MG since it has a complex morphology that combines the characteristics of glioblastoma and astrocytoma cells.

In a recent study, researchers investigated the effects of 2.4 GHz RF-EMF on the proliferation and morphology of U118-MG glioblastoma cells. The study demonstrated a notable reduction in cell viability, particularly after 72 h of RF exposure (Nowak-Terpiłowska et al. 2023). While this research predominantly addressed cell proliferation and morphological changes, without delving into the underlying molecular mechanisms. In comparison, our study examines the time-dependent effects of 2.1 GHz RF-EMF exposure, focusing on key apoptotic markers such as *CASP3, CASP8, CASP9*, and the *BAX/BCL-2* ratio. By investigating apoptosis at a molecular level, we aim to provide further insights into how RF-EMF influences apoptotic markers across varying exposure durations, thereby enhancing our understanding of the mechanisms driving RF-EMF-induced cell death.

1521186x, 2025, 1, Downloaded from https://onlinelibrary.wiley.com/doi/10.1002/bem.22543 by University Of British Columbia, Wiley Online Library on [10/10/2026]. See the Terms and Conditions (https://onlinelibrary.wiley.com/terms-and-conditions) on Wiley Online Library for rules of use; OA articles are governed by the applicable Creative Commons License

After the IARC classified radiofrequency radiation (RFR) as a probable human carcinogen (Baan et al. 2011), subsequent studies conducted by the Ramazzini Institute (RI) and the National Toxicology Program (NTP) further reported an association between RFR and glial cancer cells (Falcioni et al. 2018; Wyde et al. 2016). These studies, recognized as the largest and most extensive long-term investigations in rats concerning the health effects of RFR, played a significant role in the decision to use the glioblastoma cell line in our study. In addition, to ensure that our research reflects real-life environments, we designed and manufactured an exposure system capable of exposing cell cultures to a cell phone-specific RF field with a SAR of 1 W/kg and a frequency of 2.1 GHz. This SAR value corresponds to the average SAR emitted by a typical cell phone during usage.

Previous studies have produced inconsistent findings when evaluating the impact of RF field exposure on the proliferation of glial-based cell cultures. Some studies report increased cell proliferation (Pérez-Castejón et al. 2009), others observe a decrease (Cao et al. 2009), and some find no significant change (Kang et al. 2014; Miyakoshi et al. 2005). For instance, Liu et al. conducted two separate studies at 1950 MHz, applying the same exposure conditions to different cell lines. While an effect on rat astrocyte cells was observed in one study (Liu et al. 2012), no significant effects were found in U251 and U87 glioblastoma cells in the other (Liu et al. 2015). Similarly, different results were obtained despite the same exposure systems and conditions applied to cell lines from different donors, highlighting the complexity of the interaction between cells and RF field exposure (Nylund and Leszczynski 2006).

On the other hand, although Kang (Kang et al. 2014) and French (French, Donnellan, and McKenzie 1997) used the same cell line (U87) and close RF field exposure frequencies, they also found different results. This discrepancy can be attributed to the modulation differences, the RF application time, the difference in the RF field dose, or the use of different RF field exposure systems. Stagg et al. observed no statistically significant response of cell proliferation to RF field exposure in rat glioma C6 cells and rat astrocyte cells (Stagg et al. 1997). However, Cao et al. observed that the 900 MHz RF field significantly decreased cell viability in human astrocytoma cells (SHG44) depending on the RF dose (Cao et al. 2009). In our study, we observed that 1- and 24-h RF field exposures did not yield any significant effects on the viability of U118-MG cells, while a 48-h exposure significantly reduced cell viability compared to sham groups. These findings highlight the complexity of the relationship between RF exposure time and cell behavior and the fact that responses may vary in different cell lines.

Apoptosis, a highly regulated mechanism of cell signaling, is triggered through two main pathways: the extrinsic pathway involving the death receptors and the intrinsic mitochondrial pathway. Once inactive pro-caspases activate caspases 8 and 9, the two pathways converge with the activation of the executioner caspases (caspases 3, 6, and 7) (Singh, Letai, and Sarosiek 2019). The impact of RF fields on cell viability and apoptosis remains controversial. While previous studies have reported RF-induced apoptosis in glial-originated cell cultures (Cao et al. 2009; Pérez-Castejón et al. 2009), others have found no significant change (Hirose et al. 2006; Terro et al. 2012). In our investigation, we observed a statistically significant increase in apoptosis after 48 h of exposure to a 2.1 GHz RF field, consistent with cell viability. However, no apoptotic effect was identified after 1 or 24 h of RF exposure in U118-MG cells, underscoring the time-dependent nature of the apoptotic response in this specific cell line. This delayed effect at 48 h may be attributed to the RF exposure duration surpassing the doubling time of U118 MG cells.

Regarding the effect of RF field exposure on apoptosis-related genes, for instance, a study found a significant increase in *BAX* expression coupled with a significant decrease in *BCL-2* levels (Liu et al. 2012). Similarly, another study highlighted a significant rise in the expression of genes such as *CASP2, CASP6*, and *BAX* (Zhao, Zou, and Knapp 2007). These findings indicate that RF field exposure can influence the mRNA levels of apoptosis-related genes in astrocyte cells. However, it is essential to note that there are contrasting studies that have suggested a non-apoptotic effect of RF field exposure within the mobile phone-specific frequency range. These studies have been conducted on different glioma cell lines and have explored various exposure durations. For example, investigations on the U87 glioblastoma cell lines (1.9 GHz, 4 h RF) (Qutob et al. 2006) and SVG p12 glial cells (2.45 GHz, 1–24 h RF) (Sakurai et al. 2011) did not reveal significant changes. Similarly, glioblastoma (A172) (Hirose et al. 2006), neuroglioma (H4) (Sekijima et al. 2010), and human fibroblast (IMR-90) cell lines (Hirose et al. 2007) exhibited no significant alterations in apoptotic mRNA levels in response to the 2.1 GHz RF field. In contrast, our study demonstrated a notable observation: the *BAX/BCL-2* mRNA ratio, a crucial regulator of cellular apoptosis, showed a 4.5-fold increase in the 48 h RF exposure group compared to the sham group. Proapoptotic *BAX* can form a complex with the antiapoptotic *BCL-2*; thus, the *BAX/BCL-2* ratio determines whether a cell will undergo apoptosis, a cell death switch (Wu et al. 2021). Also, an increased *BAX/BCL-2* ratio causes the cell to undergo apoptosis by reducing its resistance to apoptotic stimuli (Schroer et al. 2023). Accordingly, in our study, the *BAX/BCL-2* ratio showed statistical significance only in the 48 h RF exposure group. This suggests the cell can tolerate apoptotic stimuli for a while but tends to undergo apoptosis after this period. The observed time-dependent differences in gene expression, particularly in apoptotic markers such as *CASP3, CASP8, CASP9*, and the *BAX/BCL-2* ratio, could be attributed to the varying stages of cellular response to RF-EMF exposure. At shorter exposure times (1 and 24 h), cells may initially activate stress response pathways, leading to early changes in gene expression, but these alterations may not immediately lead to apoptosis. Prolonged exposure (48 h) surpasses the cell's ability to cope with RF-induced stress, thus leading to significant apoptotic changes, as evidenced by the increased *BAX/BCL-2* ratio and caspase activation.

CYCD1 and *c-MYC* are both critical transcription factors in cell development, proliferation, and apoptosis (Bachnak et al. 2021), while *c-FOS*, an activator protein 1 transcription factor, is well known for its role in the regulation of cell proliferation, survival, and apoptosis (Kesarwani et al. 2017). Interestingly, after 1 h of RF exposure, *CYCD1*, *c-MYC*, and *c-FOS* expression levels were significantly increased compared to the sham groups. This

15321186x, 2025, 1, Downloaded from https://onlinelibrary.wiley.com/doi/10.1002/bem.22543 by University Of British Columbia, Wiley Online Library on [10/10/2026]. See the Terms and Conditions (https://onlinelibrary.wiley.com/terms-and-conditions) on Wiley Online Library for rules of use; OA articles are governed by the applicable Creative Commons License

immediate response may be attributed to the initial cellular response to the RF exposure, potentially induced by changes in the cellular microenvironment. Notably, despite this initial rise in transcription factor expression, no sustained changes were observed at the 24 and 48 h time points, suggesting a transient effect of RF application. The implications of this transient response need further investigation, as they may hold insights into the adaptation mechanisms of cells to prolonged RF exposure.

In light of these observations, it becomes evident that the outcomes of RF field exposure experiments are influenced by various factors, such as the selection of cell lines, the specific exposure systems and conditions employed, and the differences in exposure durations. These factors collectively contribute to the contradictory results often found in the existing literature. In our study, we observed that 24 and 48 h of RF field exposure had a significant effect on the expression levels of the genes examined (*CASP3, CASP8, CASP9, BAX, BCL-2, and BAX/BCL-2* ratio). However, extending exposure times, particularly to 48 h, led to an even more pronounced upregulation of these caspase genes (*BCL-2* downregulated) and caused significant changes in the expression of the *BAX/BCL-2* ratio. These findings underscore the importance of considering exposure duration when investigating the impact of RF field exposure on gene expression within the apoptotic pathway.

5 | Conclusion

In conclusion, this study assessed the impact of RF field exposure on U118-MG human glioblastoma cells, encompassing cell viability, apoptosis, and gene expression analyses. Our findings revealed that the response of U118-MG cells to RF field exposure exhibits variability depending on the period of RF exposure. Specifically, we showed that a 48 h exposure to an RF field resulted in caspase-dependent apoptosis, with the most significant effects reported within this experimental group. One potential effect is that cells derived from astrocytes may exhibit higher susceptibility to exposure to RF fields. In addition, when exposure to the RF field exceeds the cell's doubling time, the *BAX/BCL-2* ratio in the cells increases and acts like a switch that allows apoptosis. Overall, given the nonlinear nature of EMF-biological tissue interactions, there remains ample room for further exploration and refinement in our understanding of these complex interactions.

Acknowledgments

The authors declared that no funding is associated with the study described in this article. The authors would like to thank Melek Yaman and Zubeyir Elmazoglu for their assistance during the experiment.

Conflicts of Interest

The authors declare no conflicts of interest.

References

Baan, R., Y. Grosse, B. Lauby-Secretan, et al. 2011. "Carcinogenicity of Radiofrequency Electromagnetic Fields." *Lancet Oncology* 12: 624–626.

Bachnak, L., J. Sparks, D. E. Newmire, X. F. Gonzales, and F. O. Omoruyi. 2021. "The Effect of Acute and Chronic Thermotherapy on Type 2 Diabetic Skeletal Muscle Gene Expression and Inflammatory Markers." *Biomedicines* 9: 1276.

Bhatt, C. R., M. Redmayne, M. J. Abramson, and G. Benke. 2016. "Instruments to Assess and Measure Personal and Environmental Radiofrequency-Electromagnetic Field Exposures." *Australasian Physical & Engineering Sciences in Medicine* 39: 29–42.

Boyle, P., and B. Levin. 2008. *World Cancer Report 2008*. IARC Press, International Agency for Research on Cancer.

Brauchle, E., S. Thude, S. Y. Brucker, and K. Schenke-Layland. 2014. "Cell Death Stages in Single Apoptotic and Necrotic Cells Monitored by Raman Microspectroscopy." *Scientific Reports* 4: 4698.

Cantu, J. C., J. W. Butterworth, J. A. Payne, and I. Echchgadda. 2024. "Transcriptional Response of Primary Hippocampal Neurons Following Exposure to 3.0 GHz Radiofrequency Electromagnetic Fields." *Bioelectromagnetics* 45: 348–362.

Cao, Y., W. Zhang, M. X. Lu, et al. 2009. "900-MHz Microwave Radiation Enhances γ-Ray Adverse Effects on SHG44 Cells." *Journal of Toxicology and Environmental Health, Part A* 72: 727–732.

Chauhan, V., S. S. Qutob, S. Lui, et al. 2007. "Analysis of Gene Expression in Two Human-Derived Cell Lines Exposed in Vitro to a 1.9 GHz Pulse-Modulated Radiofrequency Field." *Proteomics* 7: 3896–3905.

Falcioni, L., L. Bua, E. Tibaldi, et al. 2018. "Report of Final Results Regarding Brain and Heart Tumors in Sprague-Dawley Rats Exposed From Prenatal Life Until Natural Death to Mobile Phone Radiofrequency Field Representative of a 1.8 GHz GSM Base Station Environmental Emission." *Environmental Research* 165: 496–503.

French, P. W., M. Donnellan, and D. R. McKenzie. 1997. "Electromagnetic Radiation at 835 MHz Changes the Morphology and Inhibits Proliferation of a Human Astrocytoma Cell Line." *Bioelectrochemistry and Bioenergetics* 43: 13–18.

de Gannes, F. P., E. Haro, A. Hurtier, et al. 2011. "Effect of Exposure to the Edge Signal on Oxidative Stress in Brain Cell Models." *Radiation Research* 175: 225–230.

Georgiou, C. D., and L. H. Margaritis. 2021. "Oxidative Stress and NADPH Oxidase: Connecting Electromagnetic Fields, Cation Channels and Biological Effects." *International Journal of Molecular Sciences* 22: 10041.

Hao, Y., W. Liu, Z. Xu, et al. 2022. "High-Power Electromagnetic Pulse Exposure of Healthy Mice: Assessment of Effects on Mice Cognitions, Neuronal Activities, and Hippocampal Structures." *Frontiers in Cellular Neuroscience* 16: 898164.

Hardell, L., M. Carlberg, and K. Hansson Mild. 2013. "Use of Mobile Phones and Cordless Phones Is Associated With Increased Risk for Glioma and Acoustic Neuroma." *Pathophysiology* 20: 85–110.

Hirose, H., N. Sakuma, N. Kaji, et al. 2006. "Phosphorylation and Gene Expression of p53 Are Not Affected in Human Cells Exposed to 2.1425 GHz Band CW or W-CDMA Modulated Radiation Allocated to Mobile Radio Base Stations." *Bioelectromagnetics* 27: 494–504.

Hirose, H., N. Sakuma, N. Kaji, et al. 2007. "Mobile Phone Base Station-Emitted Radiation Does Not Induce Phosphorylation of Hsp27." *Bioelectromagnetics* 28: 99–108.

IEC/IEEE International Standard. 2020. "Measurement Procedure for the Assessment of Specific Absorption Rate of Human Exposure to Radio Frequency Fields From Hand-Held and Body-Mounted Wireless Communication Devices." In *Part 1528: Human Models, Instrumentation, and Procedures (Frequency Range of 4 MHz to 10 GHz)*, 1–284, 19 Oct. IEC/IEEE 62209-1528:2020. https://doi.org/10.1109/IEEESTD.2020.9231298.

Joushomme, A., A. Garenne, M. Dufossée, et al. 2022. "Label-Free Study of the Global Cell Behavior during Exposure to Environmental Radiofrequency

1521186x, 2025, 1, Downloaded from https://onlinelibrary.wiley.com/doi/10.1002/bem.22543 by University Of British Columbia, Wiley Online Library on [10/10/2026]. See the Terms and Conditions (https://onlinelibrary.wiley.com/terms-and-conditions) on Wiley Online Library for rules of use; OA articles are governed by the applicable Creative Commons License

Fields in the Presence or Absence of Pro-Apoptotic or Pro-Autophagic Treatments." *International Journal of Molecular Sciences* 23: 658.

Kang, K. A., H. C. Lee, J. J. Lee, et al. 2014. "Effects of Combined Radiofrequency Radiation Exposure on Levels of Reactive Oxygen Species in Neuronal Cells." *Journal of Radiation Research* 55: 265–276.

Kayhan, H., M. A. Esmekaya, A. S. Y. Saglam, et al. 2016. "Does MW Radiation Affect Gene Expression, Apoptotic Level, and Cell Cycle Progression of Human SH-SY5Y Neuroblastoma Cells?" *Cell Biochemistry and Biophysics* 74: 99–107.

Kesarwani, M., Z. Kincaid, A. Gomaa, et al. 2017. "Targeting c-FOS and DUSP1 Abrogates Intrinsic Resistance to Tyrosine-Kinase Inhibitor Therapy in BCR-ABL-Induced Leukemia." *Nature Medicine* 23: 472–482.

Lahkola, A., A. Auvinen, J. Raitanen, et al. 2007. "Mobile Phone Use and Risk of Glioma in 5 North European Countries." *International Journal of Cancer* 120: 1769–1775.

Liu, Y., G. Li, X. Fu, et al. 2015. "Exposure to 3G Mobile Phone Signals Does Not Affect the Biological Features of Brain Tumor Cells." *BMC Public Health* 15: 764.

Liu, Y., J. Tai, G. Li, et al. 2012. "Exposure to 1950-MHz TD-SCDMA Electromagnetic Fields Affects the Apoptosis of Astrocytes Via Caspase-3-Dependent Pathway." *PLoS One* 7: e42332.

Livak, K. J., and T. D. Schmittgen. 2001. "Analysis of Relative Gene Expression Data Using Real-Time Quantitative PCR and the 2−ΔΔCT Method." *Methods* 25: 402–408.

Lu, Y., M. He, Y. Zhang, et al. 2014. "Differential Pro-Inflammatory Responses of Astrocytes and Microglia Involve STAT3 Activation in Response to 1800 MHz Radiofrequency Fields." *PLoS One* 9: e108318.

Miyakoshi, J., K. Takemasa, Y. Takashima, G. R. Ding, H. Hirose, and S. Koyama. 2005. "Effects of Exposure to a 1950 MHz Radio Frequency Field on Expression of Hsp70 and Hsp27 in Human Glioma Cells." *Bioelectromagnetics* 26: 251–257.

Nowak-Terpiłowska, A., R. Górski, M. Marszałek, et al. 2023. "Effects of 2.4 GHz Radiofrequency Electromagnetic Field (RF-EMF) on Glioblastoma Cells (U-118 MG)." *Annals of Agricultural and Environmental Medicine* 30: 763–772.

Nylund, R., and D. Leszczynski. 2006. "Mobile Phone Radiation Causes Changes in Gene and Protein Expression in Human Endothelial Cell Lines and the Response Seems to Be Genome-And Proteome-Dependent." *Proteomics* 6: 4769–4780.

Overholt, T. L., C. Ross, R. J. Evans, and S. J. Walker. 2019. "Pulsed Electromagnetic Field Therapy as a Complementary Alternative for Chronic Pelvic Pain Management in an Interstitial Cystitis/Bladder Pain Syndrome Patient." *Case Reports in Urology* 2019, no. 1: 1–3.

Pérez-Castejón, C., R. N. Pérez-Bruzón, M. Llorente, et al. 2009. "Exposure to ELF-Pulse Modulated X Band Microwaves Increases in Vitro Human Astrocytoma Cell Proliferation." *Histology and Histopathology* 24: 1551–1561.

Qutob, S. S., V. Chauhan, P. V. Bellier, et al. 2006. "Microarray Gene Expression Profiling of a Human Glioblastoma Cell Line Exposed in Vitro to a 1.9 GHz Pulse-Modulated Radiofrequency Field." *Radiation Research* 165: 636–644.

Sakurai, T., T. Kiyokawa, E. Narita, Y. Suzuki, M. Taki, and J. Miyakoshi. 2011. "Analysis of Gene Expression in a Human-Derived Glial Cell Line Exposed to 2.45 GHz Continuous Radiofrequency Electromagnetic Fields." *Journal of Radiation Research* 52: 185–192.

Schroer, J., D. Warm, F. De Rosa, H. J. Luhmann, and A. Sinning. 2023. "Activity-Dependent Regulation of the BAX/BCL-2 Pathway Protects Cortical Neurons From Apoptotic Death During Early Development." *Cellular and Molecular Life Sciences* 80: 175.

Schuderer, J., T. Samaras, W. Oesch, D. Spat, and N. Kuster. 2004. "High Peak Sar Exposure Unit With Tight Exposure and Environmental Control for in Vitro Experiments at 1800 MHz." *IEEE Transactions on Microwave Theory and Techniques* 52, no. 8: 2057–2066.

Schuermann, D., and M. Mevissen. 2021. "Manmade Electromagnetic Fields and Oxidative Stress-Biological Effects and Consequences for Health." *International Journal of Molecular Sciences* 22: 3772.

Sekijima, M., H. Takeda, K. Yasunaga, et al. 2010. "2-GHz Band CW and W-CDMA Modulated Radiofrequency Fields Have No Significant Effect on Cell Proliferation and Gene Expression Profile in Human Cells." *Journal of Radiation Research* 51: 277–284.

Senturk, F. 2023. "Hyperthermia Efficacy of PEGgylated-PLGA Coated Monodisperse Iron Oxide Nanoparticles." *Hittite Journal of Science and Engineering* 10: 153–159.

Senturk, F., S. Cakmak, I. C. Kocum, M. Gumusderelioglu, and G. G. Ozturk. 2021. "GRGDS-Conjugated and Curcumin-Loaded Magnetic Polymeric Nanoparticles for the Hyperthermia Treatment of Glioblastoma Cells." *Colloids and Surfaces, A: Physicochemical and Engineering Aspects* 622: 126648.

Shih, Y.-W., A. O'brien, C.-S. Hung, K.-H. Chen, W.-H. Hou, and H.-T. Tsai. 2020. "Exposure to Radiofrequency Radiation Increases the Risk of Breast Cancer: A Systematic Review and Meta-Analysis." *Experimental and Therapeutic Medicine* 21: 1.

Singh, R., A. Letai, and K. Sarosiek. 2019. "Regulation of Apoptosis in Health and Disease: The Balancing Act of BCL-2 Family Proteins." *Nature Reviews Molecular Cell Biology* 20: 175–193.

Stagg, R. B., W. J. Thomas, R. A. Jones, and W. R. Adey. 1997. "DNA Synthesis and Cell Proliferation in C6 Glioma and Primary Glial Cells Exposed to a 836.55 MHz Modulated Radiofrequency Field." *Bioelectromagnetics* 18: 230–236.

Stupp, R., S. Taillibert, A. Kanner, et al. 2017. "Effect of Tumor-Treating Fields Plus Maintenance Temozolomide Vs Maintenance Temozolomide Alone on Survival in Patients With Glioblastoma: A Randomized Clinical Trial." *Journal of the American Medical Association* 318, no. 23: 2306–2316.

Terro, F., A. Magnaudeix, M. Crochetet, et al. 2012. "GSM-900MHz at Low Dose Temperature-Dependently Downregulates α-Synuclein in Cultured Cerebral Cells Independently of Chaperone-Mediated-Autophagy." *Toxicology* 292: 136–144.

Tuysuz, M. F. 2014. "An Energy-Efficient Qos-Based Network Selection Scheme Over Heterogeneous WLAN–3G Networks." *Computer Networks* 75: 113–133.

Wang, J., O. Fujiwara, H. Kawai, K. Wake, and S. Watanabe. 2008. "Development and Dosimetry Analysis of a 2-GHz Whole-Body Exposure Setup for Unrestrained Pregnant and Newborn Rats." *IEEE Transactions on Microwave Theory and Techniques* 56, no. 8: 2008–2013.

Wlodkowic, D., W. Telford, J. Skommer, and Z. Darzynkiewicz. 2011. "Apoptosis and Beyond: Cytometry in Studies of Programmed Cell Death." *Methods in Cell Biology* 103: 55–98.

Wu, F., Y. Ma, J. Wang, et al. 2020. "Bleomycin A5 Suppresses Drp1-Mediated Mitochondrial Fission and Induces Apoptosis in Human Nasal Polyp-Derived Fibroblasts." *International Journal of Molecular Medicine* 47: 346–360.

Wyde, M., M. Cesta, C. Blystone, et al. 2016. "Report of Partial Findings From The National Toxicology Program Carcinogenesis Studies of Cell Phone Radiofrequency Radiation in Hsd: Sprague Dawley® SD Rats (Whole Body Exposure)." *bioRxiv*: 055699. https://doi.org/10.1101/055699.

Xu, S., G. Chen, C. Chen, et al. 2013. "Cell Type-Dependent Induction of DNA Damage by 1800 MHz Radiofrequency Electromagnetic Fields Does Not Result in Significant Cellular Dysfunctions." *PLoS One* 8: e54906.

Zhao, T. Y., S. P. Zou, and P. E. Knapp. 2007. "Exposure to Cell Phone Radiation Up-Regulates Apoptosis Genes in Primary Cultures of Neurons and Astrocytes." *Neuroscience Letters* 412: 34–38.

1521186x, 2025, 1, Downloaded from https://onlinelibrary.wiley.com/doi/10.1002/bem.22543 by University Of British Columbia, Wiley Online Library on [10/10/2026]. See the Terms and Conditions (https://onlinelibrary.wiley.com/terms-and-conditions) on Wiley Online Library for rules of use; OA articles are governed by the applicable Creative Commons License

Zielinski, J., A. D. Ducray, A. M. Moeller, M. Murbach, N. Kuster, and M. Mevissen. 2020. "Effects of Pulse-Modulated Radiofrequency Magnetic Field (RF-EMF) Exposure on Apoptosis, Autophagy, Oxidative Stress and Electron Chain Transport Function in Human Neuroblastoma and Murine Microglial Cells." *Toxicology In Vitro* 68: 104963.

Supporting Information

Additional supporting information can be found online in the Supporting Information section.

1521186x, 2025, 1, Downloaded from https://onlinelibrary.wiley.com/doi/10.1002/bem.22543 by University Of British Columbia, Wiley Online Library on [10/10/2026]. See the Terms and Conditions (https://onlinelibrary.wiley.com/terms-and-conditions) on Wiley Online Library for rules of use; OA articles are governed by the applicable Creative Commons License